

Optimizing Entanglement in Nanomechanical Resonators through Quantum Squeezing and Parametric Amplification

Muhdin Abdo Wodedo,¹ Tesfay Gebremariam Tesfahannes,^{2,*} Tewodros Yirgasewa Darge,¹ and Berihu Teklu^{3,4,†}

¹*Department of Applied Physics, Adama Science and Technology University, 1888, Adama, Ethiopia.*

²*Department of Physics, Arba Minch University, 21, Arba Minch, Ethiopia.*

³*College of Computing and Mathematical Sciences, Khalifa University, 127788, Abu Dhabi, United Arab Emirates.*

⁴*Center for Cyber-Physical Systems (C2PS), Khalifa University, Abu Dhabi 127788, United Arab Emirates.*

(Dated: November 19, 2024)

We propose a scheme that optimizes entanglement in nanomechanical resonators through quantum state transfer of squeezed fields assisted by radiation pressure. The system is driven by red-detuned laser fields, which enable simultaneous cooling of the mechanical resonators while facilitating the transfer of quantum states in a weak coupling, sideband-resolved regime. The mechanical entanglement is quantified using logarithmic negativity within the bipartite Gaussian states of the two mechanical modes. Our results show that the degree of mechanical entanglement is strongly influenced by several key parameters, including the parametric phase and nonlinear gain of the non-degenerate OPA, the squeezing strength of the injected squeezed vacuum reservoir, optomechanical cooperativity (controlled by laser drive power), and the mechanical bath temperature (phonon thermal excitation). Additionally, our results indicate that careful tuning of these parameters can enhance entanglement robustness, suggesting that this optomechanical scheme holds promise for applications in quantum sensing and information processing.

I. INTRODUCTION

Entanglement is one of the most important quantum resources among quantum correlations [1], and it can be experimentally demonstrated [2–4]. It measures the non-classical effects with various features essential in quantum information processing [5–8]. In recent decades, several investigations have shown considerable attention for entanglement in microscopic and mesoscopic systems [9–12]. The utilization of quantum entanglement encompasses quantum communication [13, 14], quantum teleportation [15], quantum cryptography [16], quantum metrology [17–23], and quantum computing [24].

In recent years at mesoscopic and macroscopic systems, cavity optomechanics via radiation pressure has become a crucial candidate to capture macroscopic quantum effects with different applications [25–28]. These quantum effects are highly probable within a system through refrigeration of mechanical vibrations[29]. Utilizing resonance effect to an optical cavity array with one oscillating end mirror aids in investigating long-distance optimal optomechanical-entanglement transfer [30]. Moreover, a recent experimental demonstration of electro-mechanical entanglement in a system with a massive membrane [31], and entanglement in two massive mechanical oscillators coupled by a common cavity [32] had been realized. Indeed, there have been numerous studies conducted on the potential to entangle two mechanical oscillators via driving classical [33–35] and non-classical state of light fields [36–41]. Moreover, it is possible to entangle two mechanical oscillators via modulated optomechanical systems [42, 43], two-tone driving [44], joint effect of coherent feedback and two-tone driving [45, 46]. In addition, several hybrid optomechanical schemes have been reported to enhance the degree of entanglement in

the two oscillating mirrors, such as a Coulomb interacted oscillators involving ensemble of two-level atoms [47], a gain medium with three-level cascaded atom in doubly resonant optomechanical cavity [48–51], utilizing single-atom Raman laser [52]. More recently, entangling a distant membrane and phonon modes in a hybrid opto-magno-mechanical system [53] have been investigated theoretically.

Nonlinear crystal media have long been well-known as sources of non-classical light. Recently, Li *et al.* employed a coupled Kerr medium with an optical parametric amplifier (OPA)[54] to enhance the entanglement of two mechanical oscillators. Moreover, mechanical entanglement between two mechanical resonators in a cavity optomechanical system that contains OPA has been realized [55–57]. Other researchers [58] have analyzed the impact of a non-degenerate OPA on the cavity and mirror entanglement in optomechanical systems with strong coupling. Most recently, generation squeezed and non-classical effects in two mechanical resonators coupled to a doubly resonant cavity with non-degenerate parametric amplification have been addressed [59, 60]. Hence, incorporating a parametric amplifier in an optomechanical cavity is found to be a current research area and an efficient way of quantum state transfer to mechanical resonators. With this motivation and a recent interest in entangling mechanical resonators, whether in a doubly resonant cavity with intacavity non-degenerate OPA and an injected two-mode squeezed vacuum field can transfer the quantum features to two mechanical resonators through radiation pressure. This question is motivated by the recent interest in entanglement generation and multi-mode investigations of light entanglement enhancement by coupling nonlinear optical cavities.

In this work, we propose a scheme for enhancing mechanical entanglement through reservoir engineering and parametric amplification within an optomechanical framework. Specifically, we study a hybrid optomechanical system comprising a non-degenerate optical parametric amplifier (OPA) embedded in a driven, doubly resonant cavity coupled to two me-

* tesfaye.gebremariam@amu.edu.et

† berihu.gebrehiwot@ku.ac.ae

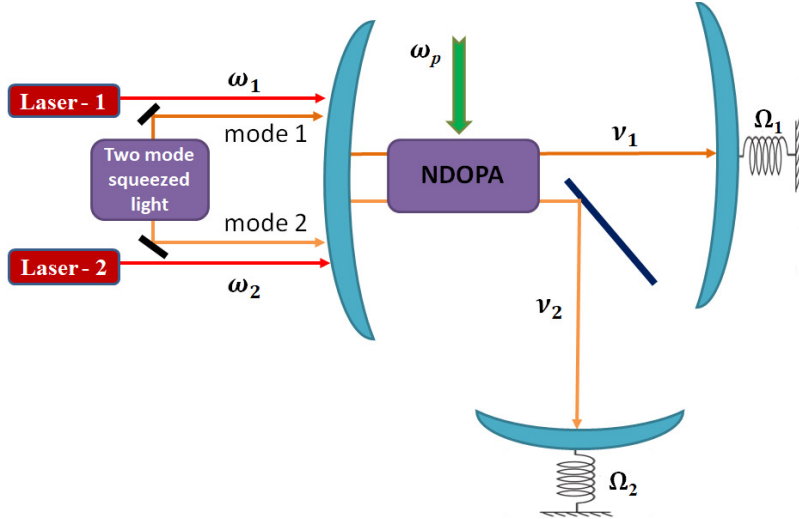


FIG. 1. The scheme of the model with a doubly resonant optomechanical cavity system comprises of a pumped intracavity non-degenerate optical parametric amplifier, a two-mode squeezed light source, and two coherent laser drives. The details of the description are in the main text.

chanical oscillators via radiation pressure. Additionally, the cavities are injected with a broadband two-mode squeezed vacuum reservoir. Our focus is on how the non-degenerate OPA and the two-mode squeezed vacuum reservoir influence the entanglement of the mechanical oscillators when the system operates in a weak coupling, sideband-resolved regime with red-detuned laser drives and resonant cavity-squeezed fields. We use logarithmic negativity to quantify continuous-variable (CV) entanglement within the bipartite Gaussian states of the two mechanical modes. The analysis shows that the degree of entanglement between the two movable mirrors is significantly influenced by critical parameters such as the parametric phase and nonlinear gain of the non-degenerate OPA, the squeezing strength of the injected squeezed vacuum reservoir, optomechanical cooperativity (controlled by laser drive power), and the mechanical bath temperature (phonon thermal excitation). Furthermore, the system under our investigation is believed to have a platform to realize quantum sensing and information processing.

The structure of this paper is as follows. In Sec. II, the Hamiltonian of the model and its dynamics including the quantum Langevin equations of mechanical modes in adiabatic approximation regime up to the covariance matrix elements from the Lyapunov equation are derived. In Sec. III, the generated entanglement between the movable mirrors with their discussion is offered. Concluding remarks are given in Sec. IV, and certain analytical results that complete the main text are given in Appendix A.

II. MODEL AND DYNAMICS OF THE SYSTEMS

We consider a dispersive hybrid optomechanical system as shown in Fig. 1, with a doubly resonant Fabry-Pérot cavity with a port fixed mirror and two completely reflecting nanomechanical mirrors. Each of the cavities in the system is

driven by two coherent lasers of frequencies ω_1 and ω_2 . Moreover, a broadband two-mode squeezed vacuum light is injected with the cavities at the fixed mirror. In addition, the non-degenerate optical parametric amplifier (NDOPA) is pumped at a frequency ω_p which is down-converted into polarization non-degenerate correlated signal and idler photon pairs with frequencies ν_1 and ν_2 . These frequencies are resonant with the corresponding cavity modes of frequencies such that an optimal transfer of the correlations in the signal-idler photon pair to the movable mirrors can be achieved [61]. We also consider that the movable mirrors are oscillating at frequencies Ω_1 and Ω_2 . Thus, the total Hamiltonian $\hat{\mathcal{H}}$ of the hybrid system described as [2, 62]

$$\hat{\mathcal{H}} = \hat{\mathcal{H}}_o + \hat{\mathcal{H}}_m + \hat{\mathcal{H}}_{om} + \hat{\mathcal{H}}_d + \hat{\mathcal{H}}_p, \quad (1)$$

where $\hat{\mathcal{H}}_o = \sum_{j=1}^2 \hbar \nu_j \hat{c}_j^\dagger \hat{c}_j$ and $\hat{\mathcal{H}}_m = \sum_{j=1}^2 \hbar \Omega_j \hat{d}_j^\dagger \hat{d}_j$ are the free Hamiltonian of the cavities and moving mirrors respectively with $\hat{c}_j(\hat{d}_j)$ and $\hat{c}_j^\dagger(\hat{d}_j^\dagger)$ describe the annihilation and creation operators of each cavity (mechanical) which satisfy the commutation relation $[\hat{O}_j, \hat{O}_{j'}] = [\hat{O}_j^\dagger, \hat{O}_{j'}^\dagger] = 0$, $[\hat{O}_j, \hat{O}_{j'}^\dagger] = \delta_{jj'}$ with $\hat{O} = \hat{c}, \hat{d}$, and $j, j' = 1, 2$. The third term $\hat{\mathcal{H}}_{om} = -\sum_{j=1}^2 \hbar g_j \hat{c}_j^\dagger \hat{c}_j (\hat{d}_j^\dagger + \hat{d}_j)$ is the optomechanical interaction Hamiltonian due to radiation pressure with $g_j = \frac{\nu_j}{L_j} \sqrt{\frac{\hbar}{2m_j \Omega_j}}$ is the single-photon optomechanical coupling with L_j is the effective length of each cavity and m_j is the effective mass of each mechanical mirror. The fourth term $\hat{\mathcal{H}}_d = \sum_{j=1}^2 i\hbar (\mathcal{E}_j e^{-i\omega_j t} \hat{c}_j^\dagger - \mathcal{E}^* e^{i\omega_j t} \hat{c}_j)$ is the Hamiltonian due to the interaction of the coherent laser driving fields and their corresponding cavity modes with $\mathcal{E}_j = |\mathcal{E}_j| e^{-i\phi_j}$, ϕ_j is the phase of laser drive, $|\mathcal{E}_j| = \sqrt{\frac{\kappa_j \mathcal{P}_j}{\hbar \omega_j}}$ is the magnitude of amplitude of driving laser which is related to the cavity driving laser power \mathcal{P}_j and the cavity decay rate κ_j . The last term $\hat{\mathcal{H}}_p = i\hbar \Lambda (e^{i\theta} e^{-i\omega_p t} \hat{c}_1^\dagger \hat{c}_2^\dagger - e^{-i\theta} e^{i\omega_p t} \hat{c}_1 \hat{c}_2)$ is the Hamiltonian of the phase-sensitive type-II polarization non-degenerate

optical parametric amplifier and the cavity modes with Λ is the non-linear parametric gain, which is proportional to the amplitude of its classical pumping field at parametric phase θ .

In a rotating frame of unitary transformation operator, $\hat{\mathcal{U}} = \exp(i\hat{\omega}_1\hat{c}_1^\dagger\hat{c}_1 t + i\hat{\omega}_2\hat{c}_2^\dagger\hat{c}_2 t)$, we obtain the Hamiltonian

$$\hat{H} = \sum_{j=1}^2 [\hbar\Delta'_j\hat{c}_j^\dagger\hat{c}_j + i\hbar(\mathcal{E}_j\hat{c}_j^\dagger - \mathcal{E}_j^*\hat{c}_j) + \hbar\Omega_j\hat{d}_j^\dagger\hat{d}_j - \hbar g_j\hat{c}_j^\dagger\hat{c}_j(\hat{d}_j^\dagger + \hat{d}_j)] + i\hbar\Lambda[\hat{c}_1^\dagger\hat{c}_2^\dagger e^{i\theta}e^{-i\Delta_p t} - \hat{c}_1\hat{c}_2 e^{-i\theta}e^{i\Delta_p t}], \quad (2)$$

where $\Delta'_j = \nu_j - \omega_j$ and $\Delta_p = \omega_p - \omega_1 - \omega_2 = \Delta'_1 + \Delta'_2$ are the detuning of cavity mode and NDOPA respectively. With the aid this equation, the dynamics of the system is described with the following set of quantum Langevin equations

$$\begin{aligned} \frac{d}{dt}\hat{d}_j &= -i\Omega_j\hat{d}_j + ig_j\hat{c}_j^\dagger\hat{c}_j - \frac{\gamma_j}{2}\hat{d}_j + \sqrt{\gamma_j}\hat{d}_j^{in}, \\ \frac{d}{dt}\hat{c}_1 &= -i\Delta'_1\hat{c}_1 + ig_1\hat{c}_1(\hat{d}_1^\dagger + \hat{d}_1) + \mathcal{E}_1 \\ &\quad + \Lambda e^{i\theta}e^{-i\Delta_p t}\hat{c}_2^\dagger - \frac{\kappa_1}{2}\hat{c}_1 + \sqrt{\kappa_1}\hat{c}_1^{in}, \\ \frac{d}{dt}\hat{c}_2 &= -i\Delta'_2\hat{c}_2 + ig_2\hat{c}_2(\hat{d}_2^\dagger + \hat{d}_2) + \mathcal{E}_2 \\ &\quad + \Lambda e^{i\theta}e^{-i\Delta_p t}\hat{c}_1^\dagger - \frac{\kappa_2}{2}\hat{c}_2 + \sqrt{\kappa_2}\hat{c}_2^{in}, \end{aligned} \quad (3)$$

where \hat{c}_j^{in} and \hat{d}_j^{in} are the annihilation operators related to input noises with zero-mean value associated with each cavity and moving mirror, respectively. We assume the mass of the movable mirrors are in nano-gram scale such that they oscillate at high-frequency associated with very high mechanical quality factors ($Q_j = \Omega_j/\gamma_j \gg 1$) and operate in ultra-cold temperatures. In this regard, the noise operator of each mirror can be taken as a Gaussian white-noise source, hence its evolution can be considered a Markovian process [63]. Thus, thermal noise operator \hat{d}_j^{in} with nonzero delta correlation functions become [64] $\langle \hat{d}_j^{in,\dagger}(t)\hat{d}_j^{in}(t') \rangle = n_j\delta(t-t')$ and $\langle \hat{d}_j^{in}(t)\hat{d}_j^{in,\dagger}(t') \rangle = (n_j+1)\delta(t-t')$, with $n_j = [\exp([\hbar\Omega_j/(k_B T_j)]-1)]^{-1}$ is the mean thermal excitation (phonon) number in the movable mirror at temperature T_j and k_B denotes the standard Boltzmann's constant. On the other hand, the quantum noise fluctuation component \hat{c}_j^{in} is assumed to be injecting a weak two-mode squeezed state with a nature of broadband width with its central frequency $\omega'_j = \nu_j$. This allows the transfer of optimal entanglement to the mechanical oscillators can be achieved [61]. Thus, the noise operator \hat{c}_j^{in} second-order non-zero correlation functions can be described as $\langle \hat{c}_j^{in,\dagger}(t)\hat{c}_j^{in}(t') \rangle = \mathcal{N}_j\delta(t-t')$, $\langle \hat{c}_j^{in}(t)\hat{c}_j^{in,\dagger}(t') \rangle = (\mathcal{N}_j+1)\delta(t-t')$, $\langle \hat{c}_j^{in}(t)\hat{c}_{j'}^{in,\dagger}(t') \rangle = \mathcal{M}\delta(t-t')$, and $\langle \hat{c}_j^{in,\dagger}(t)\hat{c}_{j'}^{in,\dagger}(t') \rangle = \mathcal{M}^*\delta(t-t')$; $j, j' = 1, 2$ ($j \neq j'$) [65, 66]. Here $\mathcal{N}_1 = \mathcal{N}_2 = \mathcal{N} = \sinh^2 r$ and $\mathcal{M} = e^{i\varphi}\cosh(r)\sinh(r)$ with r and φ are squeezing strength and phase of the squeezing respectively.

According to Eq. (3), we obtain the steady-state average

values of each operators of the system as

$$\begin{aligned} c_1^s &= \frac{2\mathcal{E}_1(\kappa_2 - 2i\Delta_2)}{(\kappa_1 + 2i\Delta_1)(\kappa_2 - 2i\Delta_2) - 4\Lambda^2}, \\ c_2^s &= \frac{2\mathcal{E}_2(\kappa_1 - 2i\Delta_1)}{(\kappa_2 + 2i\Delta_2)(\kappa_1 - 2i\Delta_1) - 4\Lambda^2}, \\ d_j^s &= \frac{2ig_j|c_j^s|^2}{\gamma_j + 2i\Omega_j}. \end{aligned} \quad (4)$$

Here we neglect the high-frequency terms in c_j^s , and the expression $\Delta_j = \Delta'_j - g_j(d_j^{s*} + d_j^s)$ is the effective cavity-laser field detuning of each optomechanical cavity caused by radiation pressure. Furthermore, we express each operator of the system as a zero mean quantum fluctuation $\delta\hat{O}_j$ plus the steady state value $\mathcal{O}_j^s = \langle \hat{O}_j^s \rangle$ such that $\hat{O}_j = \mathcal{O}_j^s + \delta\hat{O}_j$. Thus, the fluctuations can be easily found analytically through the linearization approach utilization [62, 67], given that the nonlinear effect found between the cavity field and the movable mirrors is assumed to be weak. The linearized form of the quantum fluctuations Langevin equations of Eq. (3) on the base of various working regimes are provided in Eq. (A1), Eq. (A2) and Eq. (A3).

Furthermore, the dynamics can be considered adiabatically in the resolved sideband regime for a high mechanical quality factor ($\Omega_j \gg \kappa_j \gg \gamma_j$) and in a very weak coupling limit ($\mathcal{G}_j \ll \kappa_j$). Thus, in such conditions, the cavity mode dynamics can follow the mechanical modes, and we can eliminate the cavity mode dynamics such that the photons leave the cavity with a lower interaction with the moving mirrors, allowing an optimal quantum state transfer [37, 61]. In this regard, we can set in large time approximation that the time rate of each of the cavity modes fluctuation operators set $\frac{d}{dt}\delta\tilde{c}_j = 0$ in Eq. (A3). Thus, we obtain the linearized dynamical quantum Langevin equations as if the system with two movable mirrors as

$$\begin{aligned} \frac{d}{dt}\delta\tilde{d}_1 &= -\frac{\Upsilon_1}{2}\delta\tilde{d}_1 + \chi\delta\tilde{d}_2^\dagger + \sqrt{\Upsilon_1}\tilde{D}_1^{in}, \\ \frac{d}{dt}\delta\tilde{d}_2 &= -\frac{\Upsilon_2}{2}\delta\tilde{d}_2 + \chi\delta\tilde{d}_1^\dagger + \sqrt{\Upsilon_2}\tilde{D}_2^{in}. \end{aligned} \quad (5)$$

Here the effective damping rate of the j^{th} mechanical mode is $\Upsilon_j = \gamma_j + \Gamma_j$ with γ_j is intrinsic damping rate, and $\Gamma_j = \frac{\mathcal{G}_j^2\kappa_j}{\mathcal{K}}$ is optically-induced damping rate for $\mathcal{K} = \frac{\kappa_1\kappa_2}{4} - \Lambda^2$, $\chi = \frac{\mathcal{G}_1\mathcal{G}_2}{\mathcal{K}}\Lambda e^{i\theta}$ is the effective coupling strength between the two mechanical modes induced by the driving lasers and NDOPA, and $\tilde{D}_1^{in} = (a_1\sqrt{\kappa_1}\tilde{c}_1^{in} + b_1\sqrt{\kappa_2}\tilde{c}_2^{in,\dagger} + \sqrt{\gamma_1}\tilde{d}_1^{in})/\sqrt{\Upsilon_1}$, $\tilde{D}_2^{in} = (a_2\sqrt{\kappa_2}\tilde{c}_2^{in} + b_2\sqrt{\kappa_1}\tilde{c}_1^{in,\dagger} + \sqrt{\gamma_2}\tilde{d}_2^{in})/\sqrt{\Upsilon_2}$ are the effective noise operator to the respective movable mirrors with $a_1 = \frac{i\mathcal{G}_1\kappa_2}{2\mathcal{K}}$, $b_1 = \frac{i\mathcal{G}_1\Lambda e^{i\theta}}{\mathcal{K}}$, $a_2 = \frac{i\mathcal{G}_2\kappa_1}{2\mathcal{K}}$, $b_2 = \frac{i\mathcal{G}_2\Lambda e^{i\theta}}{\mathcal{K}}$. Thus, in the presence of the NDOPA ($\Lambda \neq 0$) and the cavity driving laser field ($\mathcal{G}_j \neq 0$), it is noted that, $\frac{d}{dt}\delta\tilde{d}_j$ depends on $\delta\tilde{d}_j^\dagger$, and $\tilde{c}_j^{in,\dagger}$ that implies the two movable mirrors undergoes parametric down conversion interaction. Therefore, the NDOPA in the system or the squeezed noise injection can cause entanglement between the two movable mirrors.

Following this, we write the operators in Eq. (5) in terms of quadrature operators to quantify a continuous-variable en-

tanglement between the bipartite systems. Here, we introduce quadrature operators for mechanical modes as $\delta\tilde{Q}_j = \frac{1}{\sqrt{2}}(\delta\tilde{d}_j^\dagger + \delta\tilde{d}_j)$ and $\delta\tilde{P}_j = \frac{i}{\sqrt{2}}(\delta\tilde{d}_j^\dagger - \delta\tilde{d}_j)$. Similarly, the corresponding input noise quadrature operators defined as $\tilde{Q}_j^{in} = \frac{1}{\sqrt{2}}(\tilde{D}_j^{in,\dagger} + \tilde{D}_j^{in})$ and $\tilde{P}_j^{in} = \frac{i}{\sqrt{2}}(\tilde{D}_j^{in,\dagger} - \tilde{D}_j^{in})$. Thus, the dynamical equations of the system in Eq. (5) are simplified into a compact form first-order differential equation as

$$\frac{d}{dt}\mathcal{Z}(t) = \mathcal{B}\mathcal{Z}(t) + \mathcal{S}(t), \quad (6)$$

where $\mathcal{Z}(t) = (\delta\tilde{Q}_1, \delta\tilde{P}_1, \delta\tilde{Q}_2, \delta\tilde{P}_2)^T$ is the vector of the quadrature operators, encompassing both the mechanical position and momentum fluctuations, $\mathcal{S}(t) = (\sqrt{\Upsilon_1}\tilde{Q}_1^{in}, \sqrt{\Upsilon_1}\tilde{P}_1^{in}, \sqrt{\Upsilon_2}\tilde{Q}_2^{in}, \sqrt{\Upsilon_2}\tilde{P}_2^{in})^T$ represents the vector of noise terms, which includes the contributions from the input noise quadratures, and the drift matrix, \mathcal{B} we have

$$\mathcal{B} = \begin{pmatrix} -\Upsilon_1/2 & 0 & |\chi| \cos \theta & |\chi| \sin \theta \\ 0 & -\Upsilon_1/2 & |\chi| \sin \theta & -|\chi| \cos \theta \\ |\chi| \cos \theta & |\chi| \sin \theta & -\Upsilon_2/2 & 0 \\ |\chi| \sin \theta & -|\chi| \cos \theta & 0 & \Upsilon_2/2 \end{pmatrix}. \quad (7)$$

We analyze the system's stability in Appendix Eq. (A4). Furthermore, the formal solution of the matrix equation Eq. (6) is obtained as

$$\mathcal{Z}(t) = \mathcal{Z}(0)e^{\mathcal{B}t} + \int_0^t e^{\mathcal{B}t'} \mathcal{Z}(t-t')dt', \quad (8)$$

where $\mathcal{Z}(0)$ is the vector of the initial values of the components. Since the noises \tilde{c}_j^{in} and \tilde{d}_j^{in} are δ -correlated, they describe a Markovian process. For a stable system at steady state, the covariance matrix \mathcal{R} of Eq. (A7) can therefore be determined by solving the Lyapunov equation [64].

$$\mathcal{B}\mathcal{R} + \mathcal{R}\mathcal{B}^T = -\mathcal{F}, \quad (9)$$

where \mathcal{F} is the diffusion matrix. The detailed analytic expressions of the elements of the matrices \mathcal{F} and \mathcal{R} are derived in the Appendix with the expression of their elements provided in Eq. (A5) and Eq. (A8) respectively.

III. QUANTIFICATION OF ENTANGLEMENT

A two-mode CV system's entanglement may be quantified by entanglement monotones such as entanglement negativity [68–70] and entanglement of formation [71–73]. Both may be computed starting from the covariance matrix of the system. Entanglement negativity is commonly employed as an entanglement measure for analytical simplicity. It is defined based on the minimum symplectic eigenvalue of the partially transposed covariance matrix of the Gaussian state in question. The negativity E_N is given by

$$E_N = \max[0, -\ln(2V_s)], \quad (10)$$

where V_s is the minimum symplectic eigenvalue of the partially transposed Gaussian state under investigation. In this regard,

the smallest symplectic eigenvalue V_s of the partial transpose of the 4×4 covariance matrix \mathcal{R} is found to have the form

$$V_s = \sqrt{\frac{\zeta - \sqrt{\zeta^2 - 4 \det \mathcal{R}}}{2}}, \quad (11)$$

with $\zeta = \det \mathcal{R}_1 + \det \mathcal{R}_2 - 2 \det \mathcal{R}_3$. In line with this, the two mechanical modes are said to be entangled if and only if $E_N > 0$ or $V_s < 1/2$. Accordingly, we utilize the covariance matrix elements analytical expressions of Eq. (A8), to quantify the degree of entanglement in nanomechanical resonators.

Furthermore, to realize the generation of entanglement between the mechanical modes in our scheme, we use feasible parameters based on recent experiments in the optomechanical system [74] and certain theoretical values satisfying the chosen parametric regime. For simplicity, we take identical parameters for field-mirror pairs such that the wavelength of the driving lasers $1064nm(\omega_1/2\pi = \omega_2/2\pi = 2.82 \times 10^{14}Hz)$, frequency of the mechanical oscillators $\Omega_1/2\pi = \Omega_2/2\pi = 947 \times 10^3Hz$, masses of the movable mirrors $m_1 = m_2 = 145ng$, the length of the cavities $L_1 = L_2 = 25mm$, the cavity decay rates $\kappa_1/2\pi = \kappa_2/2\pi = \kappa/2\pi = 215 \times 10^3Hz$, and the mechanical modes damping rates $\gamma_1/2 = \gamma_2/2\pi = \gamma/2\pi = 140Hz$. In addition, we consider equal mechanical bath temperatures (phonon excitations), $T_1 = T_2 = T(n_1 = n_2 = n)$, and the value of phase squeezing $\varphi = 0$. Moreover, we utilize equal laser driving powers, $\mathcal{P}_1 = \mathcal{P}_2 = \mathcal{P}$ that yield identical optomechanical coupling rates, $\mathcal{G}_1 = \mathcal{G}_2 = \mathcal{G}$. Here we define the optomechanical cooperativity as $C = \frac{4\mathcal{G}^2}{\gamma\kappa}$ that is directly proportional to \mathcal{P} . The results and discussion of the plots in Figs. 2 - 7 which illustrate mechanical entanglement dependence on the squeezing strength (r) of two-mode squeezed field injection, the parametric phase (θ) and gain of NDOPA (Λ), the thermal decoherence effect of mechanical baths (temperature T and phonon number n), and the cooperativity (C).

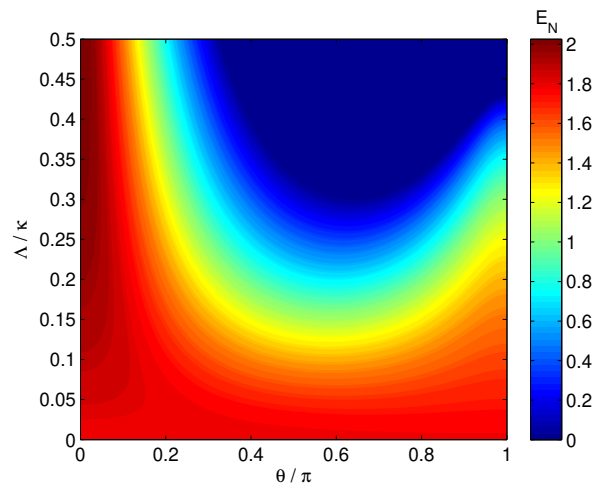


FIG. 2. Density plot of mechanical entanglement quantification (E_N) as a function of nonlinear parametric gain versus parametric phase of NDOPA when $r = 1$, $T = 42\mu K(n = 0.5)$, $\mathcal{P} = 0.3mW(C = 62.5, \mathcal{G} = 0.1\kappa)$. The other parameters are listed in the main text.

In Fig. 2, the density plot of the entanglement measure as a function of parametric nonlinear gain Λ/κ versus normalized parametric phase (θ/π) is demonstrated. In this plot, we observe that increasing the nonlinear parametric gain of NDOPA enhances the degree of entanglement at a parametric phase of $\theta = 0$. On the other hand, for higher nonlinear gain, the degree of entanglement decreases from a certain value to zero as the parametric phases increase to $\theta = \pi/2$. In contrast, lower nonlinear gains show relatively higher entanglement and satisfy the CV inseparability criteria for all ranges of parametric phases. Moreover, for lower nonlinear gains as the parametric phases increase towards $\theta = \pi/2$, the degree of entanglement decreases. At the parametric phase $\theta = \pi$, it is illustrated that the degree of entanglement is reduced as the nonlinear gains enhance.

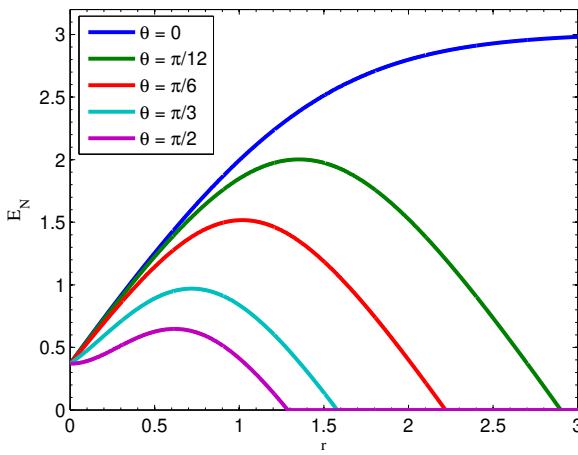


FIG. 3. Plot of Entanglement (E_N) versus squeezing strength r for different parametric phases of NDOPA when the nonlinear parametric gain $\Lambda = 0.26\kappa$. The other parameters are the same as in Fig. 2.

The entanglement versus the squeezing strength r for different parametric phases are plotted in Fig. 3. It is clearly shown that as the parametric phase increases to $\pi/2$, the degree of entanglement decreases. For $r = 0$, the entanglement values show no sensitivity for parametric phase variation. This entanglement value is due to the presence of intracavity-squeezed photons of NDOPA. Moreover, corresponding to each parametric phase as the squeezing strength increases, the degree of entanglement increases to an optimal value and then decreases except at $\theta = 0$. It is clearly shown that a wider range of the squeezing strength r of injected squeezed fields corresponded to lower values of parametric phases with enhanced entanglement. For large squeezing strength, entanglement in mechanical oscillators becomes a constant for $\theta = 0$ or starts to degrade for $\theta \neq 0$ at particular squeezing strength owing to an increasing impurity that comes from the evolution of a pure squeezed state to a thermal squeezed state [61] that increase steady-state mean phonon number (decoherence) [75].

The laser that pumps the NDOPA induces coherent superposition, which is responsible for a strong dependence of the quantum correlation properties of the radiation on the nonlinear

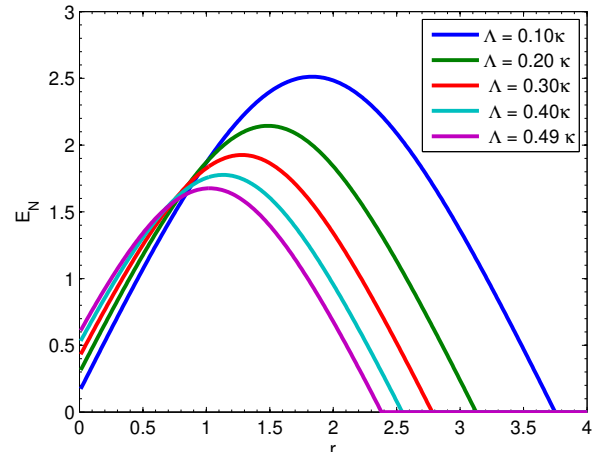


FIG. 4. Plot of Entanglement (E_N) versus squeezing strength for different parametric nonlinear gain of NDOPA when $\theta = \pi/12$. The other parameters are the same as in Fig. 2.

gain Λ proportional to the amplitude of the pumping field. In Fig. 4, in the absence of the injected squeezed vacuum fields (squeezing $r = 0$) and as the NDOPA nonlinear gain, Λ goes to zero, the mechanical modes entanglement takes the minimal value. However, in the existence of NDOPA, the generated correlated photons cause entanglement in mechanical modes for $r = 0$, and as the parametric nonlinear gain increases, the entanglement also enhances. Moreover, the joint effect of NDOPA and injected squeezed light makes the entanglement more robust in a certain limit of lower squeezing strength range, $r \neq 0$. The fact that entanglement can explain this is very directly related to the effective couplings between the two mechanical modes, χ (rely directly on the respective terms, Λ), and the correlation matrix element can be increased by squeezing strength $r = 0$ so that the entanglement becomes robust. Furthermore, the effect of NDOPA is more significant for lower squeezing strength, whereas with higher squeezing strengths, the variation of nonlinear gain of NDOPA has a negative effect. Moreover, it is over-dominated by the injected squeezed field. For considerable squeezing strength, entanglement in mechanical oscillators starts to degrade for a similar reason as in the former.

It is also essential to know the effects of the temperature of the mechanical bath, which is the resource for decoherence and diminishes entanglement. To this end, the plot of entanglement as a function of the temperature (T) of mechanical baths is shown in Figs. 5 for different squeezing strengths (r) at fixed parametric phase $\theta = 0$ and nonlinear gain near the threshold value $\Lambda = 0.49\kappa$. Here, we examine the effect of varying the squeezing strengths on the degree of entanglement quantification of mechanical modes. It is depicted that as the squeezing strength increases, the entanglement becomes more robust against temperature. It can be inferred that the higher mechanical bath temperature increases vibration and enhances phonon numbers directly related to thermal decoherence, significantly degrading the coherence vital for entanglement. Moreover, as

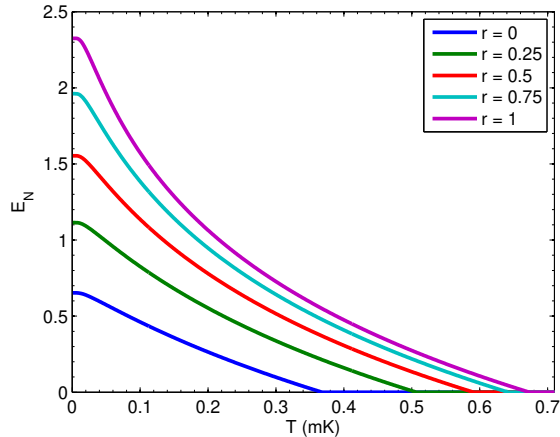


FIG. 5. Plot of Entanglement (E_N) versus temperature for different squeezing strength when NDOPA parametric phase $\theta = 0$ the nonlinear parametric gain $\Lambda = 0.49\kappa$. The other parameters are the same as in Fig. 2.

the temperature rises, the degree of entanglement diminishes for various squeezing strengths.

Moreover, the effects of optomechanical cooperativity C on the CV entanglement are plotted in Fig. 6, and Fig. 7 for different squeezing strengths r and thermal phonon numbers n , respectively. In Fig. 6 and Fig. 7, we demonstrated clearly that as the cooperativity enhanced, the degree of entanglement drastically increased for lower cooperativity values while the degree of entanglement increased slowly for higher cooperativity. It is also shown that the quantity of entanglement is enhanced due to the effect of increasing r . However increasing the phonon number n is negatively related to the degree of entanglement and thus, enhancing the phonon excitations (thermal decoherence effect) in mechanical modes is the cause

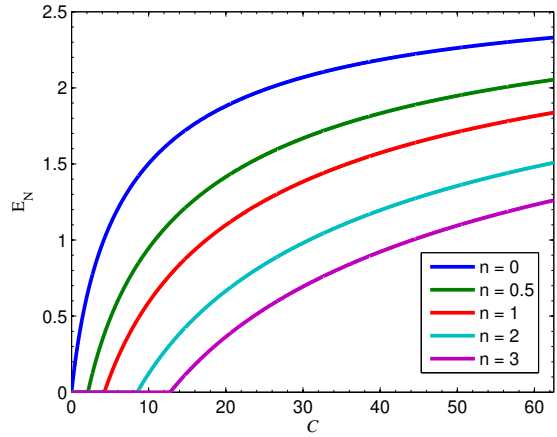


FIG. 7. Plot of Entanglement (E_N) versus cooperativity for different phonon number when NDOPA parametric phase $\theta = 0$ the nonlinear parametric gain $\Lambda = 0.49\kappa$. The other parameters are the same as in Fig. 2.

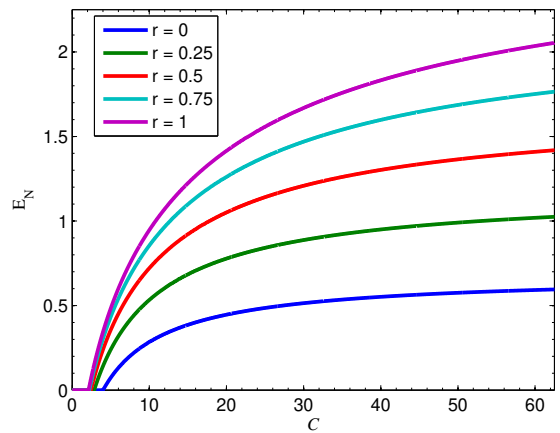


FIG. 6. Plot of Entanglement (E_N) versus cooperativity for different squeezing strength when NDOPA parametric phase $\theta = 0$ the nonlinear parametric gain $\Lambda = 0.49\kappa$. The other parameters are the same as in Fig. 2.

of the degradation of mechanical entanglement. Furthermore, the effects of cooperativity can be explained via the degree of entanglement related directly to the square of the strength of the optomechanical coupling \mathcal{G}^2 due to the radiation pressure or directly proportional to the laser driving power \mathcal{P} so that the entanglement can be enhanced. In addition, the many-photon coupling \mathcal{G} depends directly on the amplitude of the driving laser, resulting in an enhancement of intracavity photon numbers. In addition, there is a minimum cooperativity requirement to initiate entanglement in the mechanical modes corresponding to each squeezing strength in Fig. 6 and thermal phonon number in Fig. 7. In Fig. 6, it is shown that the smaller the squeezing strength, the greater the cooperativity requirement for the mechanical modes to display a non-classical effect. Similarly, in Fig. 7, the smaller the thermal phonon number corresponds to a lower quantity of cooperativity needed to attain entanglement.

In summary, regarding the entanglement generation in the nanomechanical resonators in our scheme, we illustrated logarithmic negativity as a CV entanglement measure depicted in the plots Figs. 2- 7 for the same set of parameters to the corresponding figures. These plots are shown as a function of the parametric pump phase and nonlinear gain of NOPA, the strength of the injected squeezed vacuum field, the temperature (phonon excitation) of mechanical baths, and optomechanical cooperativity. The recent experimental feasible parameters in optomechanical system [74] are relevant to realize the quantification of CV entanglement in mechanical modes theoretically. Moreover, one infers the feasibility of this quantitative entanglement found in the working regime of our scheme as in Ref.[60] by measuring the covariance matrix elements of the output cavity modes through the experimental technique suggested in Ref.[4] through two simultaneous homodyne detections.

IV. CONCLUSIONS

We have investigated the optimization of entanglement in mechanical resonators coupled through radiation pressure to a doubly resonant cavity incorporating both intra-cavity squeezed fields generated by a non-degenerate optical parametric amplifier and an extra-cavity two-mode squeezed vacuum injection. The system operates within a weak coupling, sideband-resolved regime. We used the covariance matrix elements in logarithmic negativity to quantify the entanglement of continuous-variable Gaussian bipartite states of the mechanical modes. Our findings show that the entanglement degree is significantly impacted by factors such as the squeezing strength, the phase of the parametric pump, the nonlinear gain of the non-degenerate optical parametric amplifier, optomechanical cooperativity, and the temperature of the mechanical baths. Optimal entanglement occurs at a specific phase choice where noise suppression is maximized. At this phase, increasing the squeezing parameter of the injected squeezed state further enhances entanglement robustness. Additionally, boosting the nonlinear parametric gain can strengthen the entanglement between the resonators, even at lower squeezing strengths. We also observed that coupling a two-mode squeezed vacuum reservoir to the system provides robustness against the mechanical bath's thermal noise. At higher thermal noise levels, entanglement can be enhanced by mitigating noise through increased optomechanical cooperativity. These results suggest that entanglement in the system can be controlled through various parameters, making this model a promising candidate for applications in quantum metrology and quantum information processing.

ACKNOWLEDGMENTS

BT acknowledges the support provided through the project C2PS-8474000137 and project no. 8474000739 (RIG-2024-033).

APPENDIX A

In this section for completeness, we derive the linearized form of quantum Langevin equations in rotating wave approximation, stability conditions of the system, diffusion, and covariance matrix.

For a sufficiently strong laser driving power we can assume that $|c_j^s| \gg 1$ such that the quantum Langevin equations of Eq. (3) can be safely linearized by dropping second-order quantum fluctuating terms, $\delta\hat{c}_j^\dagger\delta\hat{c}_j$, and $\delta\hat{c}_j(\delta\hat{d}_j^\dagger + \delta\hat{d}_j)$. Hence,

the dynamics of the quantum fluctuations become

$$\begin{aligned} \frac{d}{dt}\delta\hat{d}_j &= -\left(\frac{\gamma_j}{2} + i\Omega_j\right)\delta\hat{d}_j + i\mathcal{G}_j(\delta\hat{c}_2^\dagger + \delta\hat{c}_j) \\ &\quad + \sqrt{\gamma_j}\hat{d}_j^{in}, \\ \frac{d}{dt}\delta\hat{c}_1 &= -\left(\frac{\kappa_1}{2} + i\Delta_1\right)\delta\hat{c}_1 + i\mathcal{G}_1(\delta\hat{d}_1^\dagger + \delta\hat{d}_1) \\ &\quad + \Lambda e^{i\theta}e^{-i\Delta_p t}\delta\hat{c}_2^\dagger + \sqrt{\kappa_1}\hat{c}_1^{in}, \\ \frac{d}{dt}\delta\hat{c}_2 &= -\left(\frac{\kappa_2}{2} + i\Delta_2\right)\delta\hat{c}_2 + i\mathcal{G}_2(\delta\hat{d}_2^\dagger + \delta\hat{d}_2) \\ &\quad + \Lambda e^{i\theta}e^{-i\Delta_p t}\delta\hat{c}_1^\dagger + \sqrt{\kappa_2}\hat{c}_2^{in}. \end{aligned} \quad (\text{A1})$$

where $\mathcal{G}_j = g_j|c_j^s|$ is the effective optomechanical coupling rate that depends on the power \mathcal{P}_j of the input laser. Here we take the amplitude of the cavity mode c_j^s to be real via adjusting the phase ϕ_j of the laser drive field. Furthermore, we introduce slowly varying operators $\delta\tilde{c}_j = \delta\hat{c}_j e^{i\Delta_j t}$, $\tilde{c}_j^{in} = \hat{c}_j^{in} e^{i\Delta_j t}$, $\delta\tilde{d}_j = \delta\hat{d}_j e^{i\Omega_j t}$ and $\tilde{d}_j^{in} = \hat{d}_j^{in} e^{i\Omega_j t}$ into Eq. (A1), the dynamics of the linearized quantum Langevin equations become

$$\begin{aligned} \frac{d}{dt}\delta\tilde{d}_j &= -\frac{\gamma_j}{2}\delta\tilde{d}_j + i\mathcal{G}_j(\delta\tilde{c}_j^\dagger e^{i(\Delta_j + \Omega_j)t} + \delta\tilde{c}_j e^{-i(\Delta_j - \Omega_j)t}) \\ &\quad + \sqrt{\gamma_j}\tilde{d}_j^{in}, \\ \frac{d}{dt}\delta\tilde{c}_1 &= -\frac{\kappa_1}{2}\delta\tilde{c}_1 + i\mathcal{G}_1(\delta\tilde{d}_1^\dagger e^{i(\Delta_1 + \Omega_1)t} + \delta\tilde{d}_1 e^{i(\Delta_1 - \Omega_1)t}) \\ &\quad + \Lambda e^{i\theta}\delta\tilde{c}_2^\dagger + \sqrt{\kappa_1}\tilde{c}_1^{in}, \\ \frac{d}{dt}\delta\tilde{c}_2 &= -\frac{\kappa_2}{2}\delta\tilde{c}_2 + i\mathcal{G}_2(\delta\tilde{d}_2^\dagger e^{i(\Delta_2 + \Omega_2)t} + \delta\tilde{d}_2 e^{i(\Delta_2 - \Omega_2)t}) \\ &\quad + \Lambda e^{i\theta}\delta\tilde{c}_1^\dagger + \sqrt{\kappa_2}\tilde{c}_2^{in}, \end{aligned} \quad (\text{A2})$$

where we take without loss of generality for very weak coupling limit in the resolved sideband regime $\mathcal{G}_j \ll \kappa_j \ll \Omega_j$, a frequency matching can be considered such that $\Delta_p = \Delta_1 + \Delta_2$. It is also well known that when the cavity-driving beam is scattered by the vibrating cavity boundary into two portions [63, 76]. These include the first Stokes ($\omega_j - \Omega_j$) and anti-Stokes at ($\omega_j + \Omega_j$) sidebands. Subsequently, the optomechanical interaction of the field-mirror entanglement is enhanced. Our system operates at red-detuned driving lasers ($\Delta_j = \Omega_j$), wherein the cavity field and anti-Stokes scattered light are almost resonant and realize quantum state transfer to the mechanical oscillators [27, 37]. In addition, we have assumed that the mechanical quality factor is large ($\Omega_j \gg \gamma_j$), the mechanical frequency is $\Omega_j \gg \mathcal{G}_j$, and Λ the system is operating within the resolved sideband limit $\Omega_j \gg \kappa_j$. Thus, we can drop the rapid oscillating terms with $e^{2i\Omega_j t}$ in Eq. (A2) via the implementation of the rotating wave approximation (RWA). Accordingly, the the dynamics of QLEs reduced to

$$\begin{aligned} \frac{d}{dt}\delta\tilde{d}_j &= -\frac{\gamma_j}{2}\delta\tilde{d}_j + i\mathcal{G}_j\delta\tilde{c}_j + \sqrt{\gamma_j}\tilde{d}_j^{in}, \\ \frac{d}{dt}\delta\tilde{c}_1 &= -\frac{\kappa_1}{2}\delta\tilde{c}_1 + i\mathcal{G}_1\delta\tilde{d}_1 + \Lambda e^{i\theta}\delta\tilde{c}_2^\dagger + \sqrt{\kappa_1}\tilde{c}_1^{in}, \\ \frac{d}{dt}\delta\tilde{c}_2 &= -\frac{\kappa_2}{2}\delta\tilde{c}_2 + i\mathcal{G}_2\delta\tilde{d}_2 + \Lambda e^{i\theta}\delta\tilde{c}_1^\dagger + \sqrt{\kappa_2}\tilde{c}_2^{in}. \end{aligned} \quad (\text{A3})$$

To study the stability conditions of the system, we have to consider the steady-state scenario defined by Eq. (6). Particularly, the stability condition of the system can be achieved by applying the Routh-Hurwitz stability criterion [77] that confirms all the eigenvalues of the drift matrix \mathcal{B} in Eq. (7) have negative real parts. Accordingly, we derive three stability conditions for the system as

$$\begin{aligned} h_1 &= \frac{1}{4}\Upsilon_1\Upsilon_2 - |\chi|^2 > 0, \\ h_2 &= \frac{1}{4}h_1(\Upsilon_1 + \Upsilon_2)(\Upsilon_1^2 + \Upsilon_2^2 + 3\Upsilon_1\Upsilon_2 - 4|\chi|^2) > 0, \\ h_3 &= (\Upsilon_1 + \Upsilon_2)[h_2 - (\Upsilon_1 + \Upsilon_2)h_1^2] > 0. \end{aligned} \quad (\text{A4})$$

We note that the system stability conditions are independent of the parametric phase θ of the pumping field of the parametric amplifier. Furthermore, for high-quality factor mechanical oscillators with efficient laser cooling, we can take $\gamma_j \ll \Gamma_j$ [37, 61] in the system stability condition of Eq. (A4). Thus, we obtain the stability condition of the system is reduced to a more simplified form as $\Lambda < \frac{1}{2}\sqrt{\kappa_1\kappa_2}$.

Here we also derive the analytic expressions of the diffusion \mathcal{F} and covariance matrix \mathcal{R} that appeared in the Lyapunov equation Eq. (9). The diffusion matrix \mathcal{F} elements can be obtained by employing the elements of the column vector of the noise source $\mathcal{S}(t)$ and making use of the δ -correlation of the noise operators in $\mathcal{F}_{ll'}\delta(t - t') = \frac{1}{2}[\langle \mathcal{S}_l(t)\mathcal{S}_{l'}(t') \rangle + \langle \mathcal{S}_{l'}(t')\mathcal{S}_l(t) \rangle]$, ($l, l' = 1, 2, 3, 4$). Thus, the diffusion matrix takes the form

$$\mathcal{F} = \begin{pmatrix} \mathcal{F}_{11} & 0 & \mathcal{F}_{13} & \mathcal{F}_{14} \\ 0 & \mathcal{F}_{11} & \mathcal{F}_{14} & -\mathcal{F}_{13} \\ \mathcal{F}_{13} & \mathcal{F}_{14} & \mathcal{F}_{33} & 0 \\ \mathcal{F}_{14} & -\mathcal{F}_{13} & 0 & \mathcal{F}_{33} \end{pmatrix}, \quad (\text{A5})$$

with

$$\begin{aligned} \mathcal{F}_{11} &= \frac{1}{2} \left([|a_1|^2\kappa_1 + |b_1|^2\kappa_2](2\mathcal{N} + 1) \right. \\ &\quad \left. + 2[b_1^*a_1\mathcal{M} + a_1^*b_1\mathcal{M}^*]\sqrt{\kappa_1\kappa_2} + \gamma_1(2n_1 + 1) \right), \\ \mathcal{F}_{33} &= \frac{1}{2} \left([|a_2|^2\kappa_2 + |b_2|^2\kappa_1](2\mathcal{N} + 1) \right. \\ &\quad \left. + 2[b_2^*a_2\mathcal{M} + a_2^*b_2\mathcal{M}^*]\sqrt{\kappa_1\kappa_2} + \gamma_2(2n_2 + 1) \right), \\ \mathcal{F}_{13} &= \frac{1}{4} \left(([b_2^*a_1^* + b_2a_1]\kappa_1 + [b_1^*a_2^* + b_1a_2]\kappa_2)(2\mathcal{N} + 1) \right. \\ &\quad \left. + 2([b_1^*b_2^* + a_1a_2]\mathcal{M} + [b_1b_2 + a_1^*a_2^*]\mathcal{M}^*)\sqrt{\kappa_1\kappa_2} \right), \\ \mathcal{F}_{14} &= \frac{i}{4} \left(([b_2^*a_1^* - b_2a_1]\kappa_1 + [b_1^*a_2^* - b_1a_2]\kappa_2)(2\mathcal{N} + 1) \right. \\ &\quad \left. - 2([b_1^*b_2^* + a_1a_2]\mathcal{M} - [b_1b_2 + a_1^*a_2^*]\mathcal{M}^*)\sqrt{\kappa_1\kappa_2} \right). \end{aligned}$$

The stable solution for Eq. (6) is a unique solution that occurs at a steady state and is independent of the initial conditions. Since the quantum noises are zero-mean Gaussian noises and the dynamics of the fluctuations are in their linearized form, the steady-state quantum fluctuations become a zero-mean Gaussian state characterized by a 4×4 covariance matrix \mathcal{R} of the bipartite mechanical modes subsystem. The components of the covariance matrix generated from the column vector $\mathcal{Z}(t)$ at steady state (as $t \rightarrow \infty$) using $\mathcal{R}_{ll'}(\infty) = \frac{1}{2}[\langle \mathcal{Z}_l(\infty)\mathcal{Z}_{l'}(\infty) \rangle + \langle \mathcal{Z}_{l'}(\infty)\mathcal{Z}_l(\infty) \rangle]$, ($l, l' = 1, 2, 3, 4$). Further, the commutation relation between the quadrature operators in compact form as [69]

$$[\mathcal{Z}_l, \mathcal{Z}_{l'}] = i\mathcal{W}_{ll'}, \quad \mathcal{W} = \bigoplus_{l=1}^2 \begin{pmatrix} 0 & 1 \\ -1 & 0 \end{pmatrix}. \quad (\text{A6})$$

It follows that the covariance matrix \mathcal{R} of the mechanical modes becomes

$$\mathcal{R} = \begin{pmatrix} \mathcal{R}_1 & \mathcal{R}_3 \\ \mathcal{R}_3^T & \mathcal{R}_2 \end{pmatrix}, \quad (\text{A7})$$

with the 2×2 sub-block matrices, take the form $\mathcal{R}_1 = \text{diag}(\mathcal{R}_{11}, \mathcal{R}_{11})$, $\mathcal{R}_2 = \text{diag}(\mathcal{R}_{33}, \mathcal{R}_{33})$ and $\mathcal{R}_3 = \begin{pmatrix} \mathcal{R}_{13} & \mathcal{R}_{14} \\ \mathcal{R}_{14} & -\mathcal{R}_{13} \end{pmatrix}$. Here \mathcal{R}_1 and \mathcal{R}_2 describe each of the mechanical modes separately, and \mathcal{R}_3 represents the correlations between the mechanical modes. Utilizing the drift matrix \mathcal{B} of Eq. (7) and the diffusion matrix \mathcal{F} of Eq. (A5) in the Lyapunov equation Eq. (9), we obtain the analytic expressions of the elements of covariance matrix \mathcal{R} as

$$\begin{aligned} \mathcal{R}_{11} &= \frac{\det \mathcal{D}_1}{\det \mathcal{D}}, & \mathcal{R}_{13} &= \frac{\det \mathcal{D}_2}{\det \mathcal{D}}, \\ \mathcal{R}_{14} &= \frac{\det \mathcal{D}_3}{\det \mathcal{D}}, & \mathcal{R}_{33} &= \frac{\det \mathcal{D}_4}{\det \mathcal{D}}. \end{aligned} \quad (\text{A8})$$

where the matrices \mathcal{D} , \mathcal{D}_1 , \mathcal{D}_2 , \mathcal{D}_3 , and \mathcal{D}_4 are given by

$$\mathcal{D} = \begin{pmatrix} -\frac{\Upsilon_1}{2} & |\chi| \cos \theta & |\chi| \sin \theta & 0 \\ |\chi| \cos \theta & -\frac{(\Upsilon_1 + \Upsilon_2)}{2} & 0 & |\chi| \cos \theta \\ |\chi| \sin \theta & 0 & -\frac{(\Upsilon_1 + \Upsilon_2)}{2} & |\chi| \sin \theta \\ 0 & |\chi| \cos \theta & |\chi| \sin \theta & -\frac{\Upsilon_2}{2} \end{pmatrix},$$

$$\mathcal{D}_1 = \begin{pmatrix} -\frac{\mathcal{F}_{11}}{2} & |\chi| \cos \theta & |\chi| \sin \theta & 0 \\ -\mathcal{F}_{13} & -\frac{(\Upsilon_1 + \Upsilon_2)}{2} & 0 & |\chi| \cos \theta \\ -\mathcal{F}_{14} & 0 & -\frac{(\Upsilon_1 + \Upsilon_2)}{2} & |\chi| \sin \theta \\ -\frac{\mathcal{F}_{33}}{2} & |\chi| \cos \theta & |\chi| \sin \theta & -\frac{\Upsilon_2}{2} \end{pmatrix},$$

$$\mathcal{D}_2 = \begin{pmatrix} -\frac{\Upsilon_1}{2} & -\frac{\mathcal{F}_{11}}{2} & |\chi| \sin \theta & 0 \\ |\chi| \cos \theta & -\mathcal{F}_{13} & 0 & |\chi| \cos \theta \\ |\chi| \sin \theta & -\mathcal{F}_{14} & -\frac{\Upsilon_1 + \Upsilon_2}{2} & |\chi| \sin \theta \\ 0 & -\frac{\mathcal{F}_{33}}{2} & |\chi| \sin \theta & -\frac{\Upsilon_2}{2} \end{pmatrix},$$

$$\mathcal{D}_3 = \begin{pmatrix} -\frac{\Upsilon_1}{2} & |\chi| \cos \theta & -\frac{\mathcal{F}_{11}}{2} & 0 \\ |\chi| \cos \theta & -\frac{(\Upsilon_1 + \Upsilon_2)}{2} & -\mathcal{F}_{13} & |\chi| \cos \theta \\ |\chi| \sin \theta & 0 & -\mathcal{F}_{14} & |\chi| \sin \theta \\ 0 & |\chi| \cos \theta & -\frac{\mathcal{F}_{33}}{2} & -\frac{\Upsilon_2}{2} \end{pmatrix},$$

$$\mathcal{D}_4 = \begin{pmatrix} -\frac{\Upsilon_1}{2} & |\chi| \cos \theta & |\chi| \sin \theta & -\frac{\mathcal{F}_{11}}{2} \\ |\chi| \cos \theta & -\frac{(\Upsilon_1 + \Upsilon_2)}{2} & 0 & -\mathcal{F}_{13} \\ |\chi| \sin \theta & 0 & -\frac{(\Upsilon_1 + \Upsilon_2)}{2} & -\mathcal{F}_{14} \\ 0 & |\chi| \cos \theta & |\chi| \sin \theta & -\frac{\mathcal{F}_{33}}{2} \end{pmatrix}.$$

[1] R. Horodecki, P. Horodecki, M. Horodecki, and K. Horodecki, *Rev. Mod. Phys.* **81**, 865 (2009).

[2] C. Schori, J. L. Sørensen, and E. S. Polzik, *Phys. Rev. A* **66**, 033802 (2002).

[3] W. P. Bowen, R. Schnabel, P. K. Lam, and T. C. Ralph, *Phys. Rev. Lett.* **90**, 043601 (2003).

[4] J. Laurat, G. Keller, J. Oliveira-Huguenin, C. Fabre, T. Coudreau, A. Serafini, G. Adesso, and F. Illuminati, *Journal of Optics B: Quantum and Semiclassical Optics* **7**, S577 (2005).

[5] C. Silberhorn, P. K. Lam, O. Weiß, F. König, N. Korolkova, and G. Leuchs, *Phys. Rev. Lett.* **86**, 4267 (2001).

[6] S. L. Braunstein and P. van Loock, *Rev. Mod. Phys.* **77**, 513 (2005).

[7] Z.-C. Zhang, Y.-P. Wang, Y.-F. Yu, and Z.-M. Zhang, *Opt. Express* **26**, 11915 (2018).

[8] D.-G. Lai, J.-Q. Liao, A. Miranowicz, and F. Nori, *Phys. Rev. Lett.* **129**, 063602 (2022).

[9] S. Bose, K. Jacobs, and P. L. Knight, *Phys. Rev. A* **59**, 3204 (1999).

[10] V. Vedral, *New Journal of Physics* **6**, 102 (2004).

[11] B. Deb and G. S. Agarwal, *Phys. Rev. A* **78**, 013639 (2008).

[12] J. Sperling and I. A. Walmsley, *Phys. Rev. A* **95**, 062116 (2017).

[13] Z.-S. Yuan, X.-H. Bao, C.-Y. Lu, J. Zhang, C.-Z. Peng, and J.-W. Pan, *Physics Reports* **497**, 1 (2010).

[14] B. Teklu, M. Bina, and M. G. A. Paris, *Scientific Reports* **12**, 11646 (2022).

[15] J. Sherson, H. Krauter, R. Olsson, B. Julsgaard, K. Hammerer, I. Cirac, and E. Polzik, *Nature* **443**, 557 (2006).

[16] C. H. Bennett, *Phys. Rev. Lett.* **68**, 3121 (1992).

[17] G. M. D'Ariano, P. Lo Presti, and M. G. A. Paris, *Phys. Rev. Lett.* **87**, 270404 (2001).

[18] B. Teklu, S. Olivares, and M. G. A. Paris, *Journal of Physics B: Atomic, Molecular and Optical Physics* **42**, 035502 (2009).

[19] C. F. Ockeloen-Korppi, E. Damskägg, G. S. Paraoanu, F. Massel, and M. A. Sillanpää, *Phys. Rev. Lett.* **121**, 243601 (2018).

[20] V. Montenegro, M. G. Genoni, A. Bayat, and M. G. A. Paris, *Phys. Rev. Res.* **2**, 043338 (2020).

[21] A. Candeloro, S. Razavian, M. Piccolini, B. Teklu, S. Olivares, and M. G. A. Paris, *Entropy* **23**, 10.3390/e23101353 (2021).

[22] V. Montenegro, M. G. Genoni, A. Bayat, and M. G. A. Paris, *Phys. Rev. Res.* **4**, 033036 (2022).

[23] M. Asjad, B. Teklu, and M. G. A. Paris, *Phys. Rev. Res.* **5**, 013185 (2023).

[24] F. Shahandeh, A. P. Lund, and T. C. Ralph, *Phys. Rev. A* **99**, 052303 (2019).

[25] T. Kippenberg and K. Vahala, *Science (New York, N.Y.)* **321**, 1172 (2008).

[26] P. Meystre, *Annalen der Physik* **525**, 215 (2013).

[27] M. Aspelmeyer, T. J. Kippenberg, and F. Marquardt, *Rev. Mod. Phys.* **86**, 1391 (2014).

[28] C. Shang, H. Z. Shen, and X. X. Yi, *Opt. Express* **27**, 25882 (2019).

[29] D.-G. Lai, W. Qin, A. Miranowicz, and F. Nori, *Phys. Rev. Res.* **4**, 033102 (2022).

[30] C. Shang and H. Li, *Phys. Rev. Appl.* **21**, 044048 (2024).

[31] J. Li and S. Gröblacher, *New J. Phys.* **22**, 063041 (2020).

[32] C. F. Ockeloen-Korppi, E. Damskägg, J.-M. Pirkkalainen, M. Asjad, A. A. Clerk, F. Massel, M. J. Woolley, and M. A. Sillanpää, *Nature* **556**, 478 (2018).

[33] S. Pirandola, D. Vitali, P. Tombesi, and S. Lloyd, *Phys. Rev. Lett.* **97**, 150403 (2006).

[34] D. Vitali, S. Mancini, and P. Tombesi, *Journal of Physics A: Mathematical and Theoretical* **40**, 8055 (2007).

[35] Q. Lin, B. He, and M. Xiao, *Phys. Rev. Appl.* **13**, 034030 (2020).

[36] J. Zhang, K. Peng, and S. L. Braunstein, *Phys. Rev. A* **68**, 013808 (2003).

[37] M. Pinard, A. Dantan, D. Vitali, O. Arcizet, T. Briant, and A. Heidmann, *Europhysics Letters* **72**, 747 (2005).

[38] S. Huang and G. S. Agarwal, *New Journal of Physics* **11**, 103044 (2009).

[39] L. Mazzola and M. Paternostro, *Phys. Rev. A* **83**, 062335 (2011).

[40] E. A. Sete, H. Eleuch, and C. H. R. Ooi, *J. Opt. Soc. Am. B* **31**, 2821 (2014).

[41] C.-J. Yang, J.-H. An, W. Yang, and Y. Li, *Phys. Rev. A* **92**, 062311 (2015).

[42] M. Wang, X.-Y. Lü, Y.-D. Wang, J. Q. You, and Y. Wu, *Phys. Rev. A* **94**, 053807 (2016).

[43] S. Chakraborty and A. K. Sarma, *Phys. Rev. A* **97**, 022336 (2018).

[44] M. J. Woolley and A. A. Clerk, *Phys. Rev. A* **89**, 063805 (2014).

[45] J. Li, G. Li, S. Zippilli, D. Vitali, and T. Zhang, *Phys. Rev. A* **95**, 043819 (2017).

[46] R. Peng, C. Zhao, Z. Yang, J. Yang, and L. Zhou, *Phys. Rev. A* **107**, 013507 (2023).

[47] A. Sohail, M. Rana, S. Ikram, T. Munir, T. Hussain, R. Ahmed, and C.-s. Yu, *Quantum Information Processing* **19**, 372 (2020).

[48] L. Zhou, Y. Han, J. Jing, and W. Zhang, *Phys. Rev. A* **83**, 052117 (2011).

[49] W. Ge, M. Al-Amri, H. Nha, and M. S. Zubairy, *Phys. Rev. A* **88**, 022338 (2013).

[50] E. A. Sete and H. Eleuch, *J. Opt. Soc. Am. B* **32**, 971 (2015).

[51] M. Bekele, T. Yirgasewha, and S. Tesfa, *Phys. Rev. A* **107**, 012417 (2023).

[52] B. Teklu, T. Byrnes, and F. S. Khan, *Phys. Rev. A* **97**, 023829 (2018).

[53] M. Tadesse, T. G. Tesfahannes, T. Darge, M. Wodado, and H. Dagnaw, *AIP Advances* **14** (2024).

[54] J. Li, B. Hou, Y. Zhao, and L. Wei, *EPL (Europhysics Letters)* **110**, 64004 (2015).

[55] Y. Jiao, Y. Zuo, Y. Wang, W. Lu, J.-Q. Liao, L. Kuang, and H. Jing, *Laser & Photonics Reviews* (2024).

[56] H. Dagnaw, T. G. Tesfahannes, T. Darge, and A. Getahun, *Scientific Reports* **2023** (2023).

[57] J. Wei, T. Wang, S. Zhang, and H.-F. Wang, *Advanced Quantum Technologies* **7** (2024).

[58] R. Ahmed and S. Qamar, *Physica Scripta* **92**, 105101 (2017).

[59] Y. Luo and H. Tan, *Quantum Science and Technology* **5**, 045023 (2020).

- [60] M. Wodedo, T. G. Tesfahannes, T. Darge, M. Bedore, A. Getahun, and G. Adera, *Scientific Reports* **14** (2024).
- [61] K. Jähne, C. Genes, K. Hammerer, M. Wallquist, E. S. Polzik, and P. Zoller, *Phys. Rev. A* **79**, 063819 (2009).
- [62] S. Mancini and P. Tombesi, *Phys. Rev. A* **49**, 4055 (1994).
- [63] C. Genes, A. Mari, P. Tombesi, and D. Vitali, *Phys. Rev. A* **78**, 032316 (2008).
- [64] D. Vitali, S. Gigan, A. Ferreira, H. R. Böhm, P. Tombesi, A. Guerreiro, V. Vedral, A. Zeilinger, and M. Aspelmeyer, *Phys. Rev. Lett.* **98**, 030405 (2007).
- [65] C. W. Gardiner and P. Zoller, Springer-Verlag, Berlin **97**, 98 (2000).
- [66] Y. Yan, W. Gu, and G. Li, *Science China Physics, Mechanics & Astronomy* **58**, 1 (2015).
- [67] D. F. Walls and G. J. Milburn, *Quantum Optics* (Springer, Berlin, 2008).
- [68] G. Vidal and R. F. Werner, *Phys. Rev. A* **65**, 032314 (2002).
- [69] G. Adesso, A. Serafini, and F. Illuminati, *Phys. Rev. A* **70**, 022318 (2004).
- [70] M. B. Plenio, *Phys. Rev. Lett.* **95**, 090503 (2005).
- [71] C. H. Bennett, D. P. DiVincenzo, J. A. Smolin, and W. K. Wootters, *Phys. Rev. A* **54**, 3824 (1996).
- [72] G. Giedke, M. M. Wolf, O. Krüger, R. F. Werner, and J. I. Cirac, *Phys. Rev. Lett.* **91**, 107901 (2003).
- [73] P. Marian and T. A. Marian, *Phys. Rev. Lett.* **101**, 220403 (2008).
- [74] S. Groeblacher, K. Hammerer, M. Vanner, and M. Aspelmeyer, *Nature* **460**, 724 (2009).
- [75] W.-j. Gu, G.-x. Li, and Y.-p. Yang, *Phys. Rev. A* **88**, 013835 (2013).
- [76] C. Genes, D. Vitali, and P. Tombesi, *Phys. Rev. A* **77**, 050307 (2008).
- [77] E. X. DeJesus and C. Kaufman, *Phys. Rev. A* **35**, 5288 (1987).